J. Phys. IV France **11** (2001)

The phase stability of ε-Fe alloys

M. Acet, H. Herper, P. Entel and E.F. Wassermann

Tieftemperaturphysik, Gerhard-Mercator Universität Duisburg, 47048 Duisburg, Germany

Abstract. The hexagonal close packed ϵ-phase of Fe, which is of particular interest in the study of shape memory effects in some Fe-based alloys, can be stabilized in pure Fe under a pressure of about 11 GPa. Also, Fe will be in the ϵ-phase in the absence of ferromagnetic correlations in the α-phase. Therefore, an alternative to applying pressure to stabilize the ϵ-phase is to destroy the long range ferromagnetic ordering in α-Fe by alloying appropriate elements. In this study we discuss the relationship of the magnetic properties and the stability of the ϵ-phase in Fe and Fe-rich alloys with the aid of thermodynamical considerations and total energy calculations.

1. INTRODUCTION

The martensitic transformation between the face centered cubic, fcc (γ), and the hexagonal close packed, hcp (ϵ), structures in Fe alloys is currently being exploited for the possible occurrence of useful shape memory effects. The principle constituents of these alloys are Fe and Mn, and so far the most successful candidate in γ↔ϵ transformation category appears to be Fe-Mn-Si alloys, which is both inexpensive and exhibits favorable shape memory features [1-4]. The drawback of these alloys is their low resistance to corrosion which nevertheless can be overcome considerably by the addition of Cr, Ni and Co [5].

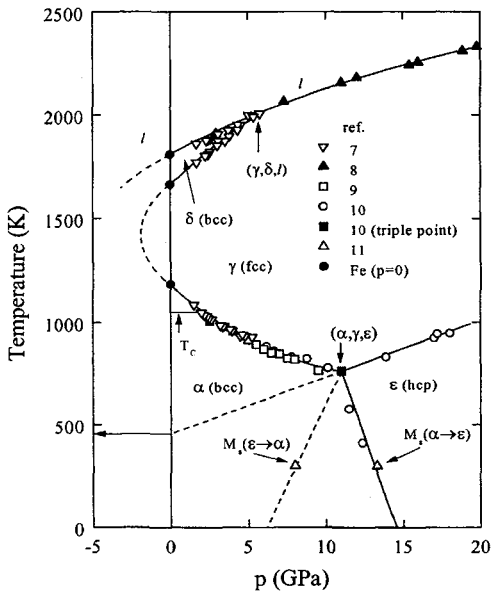

Figure 1. The p-T diagram of Fe showing the structural phase boundaries. References are numbered next to symbols.

To survey further the properties of ferrous alloys undergoing the γ↔ϵ martensitic transformation it would be useful to understand the mechanisms underlying this phase transition [6]. It may then be possible to consider other alloy alternatives or to manipulate preparation parameters that influence the shape memory effect. The question we want to address here is why Fe and Fe-rich alloys can acquire a hcp structure at all. To achieve our aim we discuss the allotropy of Fe under pressure and the relative stability of its various structural phases with relation to its magnetic properties.

2. THE p-T DIAGRAM OF Fe

The data used in the construction of the p-T diagram in figure 1 is collected from various literature [7-11]. At ambient pressure the body centered cubic (bcc) α-phase of Fe is stable below $A_3 = 1184\,K$. For $A_3 < T < A_4$ where $A_4 = 1665\,K$ the γ-phase is stable and for higher temperatures up to the melt the bcc δ-phase is stable. At the α-γ boundary the atomic volume in the low temperature α-phase is larger than

in the high temperature γ-phase. Therefore, on increasing pressure the stability of the smaller volume state is favored and the γ-region broadens. The dashed curve shows that at negative pressures the γ phase would have closed and only the α-phase would have been stable.

Around 11 GPa the ϵ-phase stabilizes at the triple point (α,γ,ϵ) and at p ≥ 15 GPa it becomes stable down to low temperatures. Since the ϵ-phase is denser packed than the γ-phase, the γ-ϵ boundary shifts towards higher temperatures with increasing pressure. From extrapolation, a hypothetical value of ~ 450 K is obtained for the γ-ϵ transformation at p=0, indicating that in the absence of the α-phase, the ϵ-phase would have been more stable than the γ phase. The α-ϵ transformation exhibits a hysteresis that broadens with decreasing temperature. The forward and reverse transformation temperatures are denoted by $M_s(\alpha \rightarrow \epsilon)$ and $M_s(\alpha \leftarrow \epsilon)$ respectively.

The boundaries between the solid and liquid (*l*) phases, δ-*l* and γ-*l*, shift to higher temperatures as the pressure is increased. The δ phase narrows with increasing pressure and eventually vanishes at the point p=5.2 GPa and T=1990 K denoted by (γ,δ,*l*). Extrapolating the γ-*l* boundary to p=0 yields a γ-phase melting temperature that is similar to that of the α-phase.

3. THE RELATIVE STABILITIES OF THE PHASES OF Fe

3.1 The Gibbs free energies

The relative stabilities of the different phases of Fe is determined by comparing their Gibbs free energies G given by

$$G(T) = H(T) - TS(T), \tag{1}$$

where the enthalpy H(T) and the entropy S(T) are respectively given as

$$H(T) = H_0 + \int_0^T c_p(T)\,dT \qquad \text{and} \qquad S(T) = S_0 + \int_0^T \frac{c_p(T)}{T}\,dT. \tag{2}$$

The specific heat at constant pressure c_p of α-Fe can be analyzed as $c_p = c_v + c_{an} + c_{el} + c_m$ where c_v, c_{an}, c_{el} and c_m are the lattice, anharmonic, electronic and magnetic contributions respectively. For γ-Fe c_m is replaced by an excess specific heat term c_{ex} which describes an excess contribution arising from the presence of strong ferromagnetic short range correlations in the γ-phase, otherwise known as the anti-Invar effect [12,13]. The specific heat analysis is dealt with in detail in references 14 and 15.

In figure 2a we compare G^α to G^γ and $G^{\gamma(NM)}$, where NM denotes "non-magnetic", implying absence of magnetic correlations due to anti-Invar effect. $G^{\gamma(NM)}$ is determined by disregarding c_{ex}. Setting H(T) of α-Fe at T=0 as $H^\alpha(0)=0$ gives $H^\gamma(0)=+5200$ J/mol implying that at T=0 α-Fe is more stable than γ-Fe by $G^\alpha - G^\gamma = -5200$ J/mol. As the temperature increases $G^\alpha - G^\gamma$ becomes smaller due to weakening magnetic order as the Curie temperature T_C is approached. For $A_3 < T < A_4$, $G^\alpha - G^\gamma > 0$ and the γ-phase is stable. For $T > A_4$ the bcc structure regains stability with the δ-phase setting in. The small value of $\Delta G \leq 100$ J/mol for $A_3 < T < A_4$ implies that small changes which can be induced in the electronic structure by eternal pressure or alloying can readily stabilize further either the α-phase or the γ-phase. The presence of the ferritic and austenitic families of Fe alloys is based on this delicate balance.

Eliminating c_m from c_p of α-Fe gives $G^{\alpha(NM)}$. The total magnetic enthalpy of α-Fe is found to be 8300 J/mol. Therefore, at T=0 $G^{\alpha(NM)} - G^\gamma = -5200 + 8300 = 3100$ J/mol. The difference decreases with increasing temperature and the curve eventually merges with the $G^\alpha - G^\gamma$ curve at $T > A_3$. This implies that α-Fe without magnetic correlations would have always been unstable with respect to the γ-phase.

The relative stability of the α and γ(NM)-phases is given with $G^\alpha - G^{\gamma(NM)}$. As the temperature is increased from low temperatures $G^\alpha - G^{\gamma(NM)}$ first increases. This indicates that there is a tendency for the stability of the α-phase to weaken due to weakening magnetic order. However, the curve then reaches a maximum at T ≈ 750 K after which it proceeds to increase negatively as the entropy increase of the α-phase exceeds that of the γ(NM)-phase. The behaviour of $G^\alpha - G^{\gamma(NM)}$ shows therefore, that the γ-phase would not have been stable without the presence of short range ferromagnetic correlations.

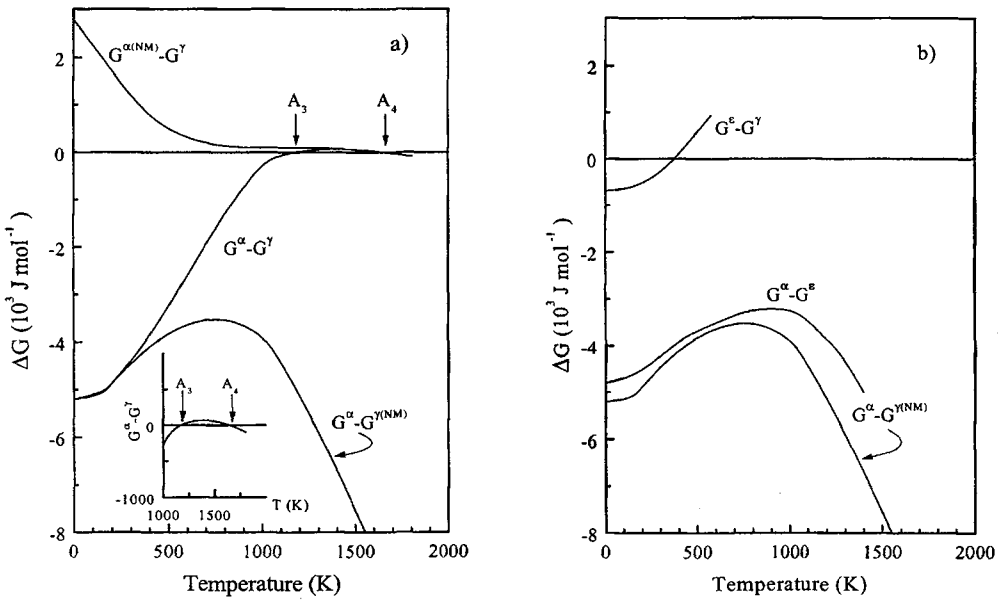

Figure 2. The temperature dependence of the differences in Gibbs free energies between a) the α and γ-phases and b) the α and ϵ-phases and of Fe. NM denotes non-magnetic implying absence of magnetic correlations.

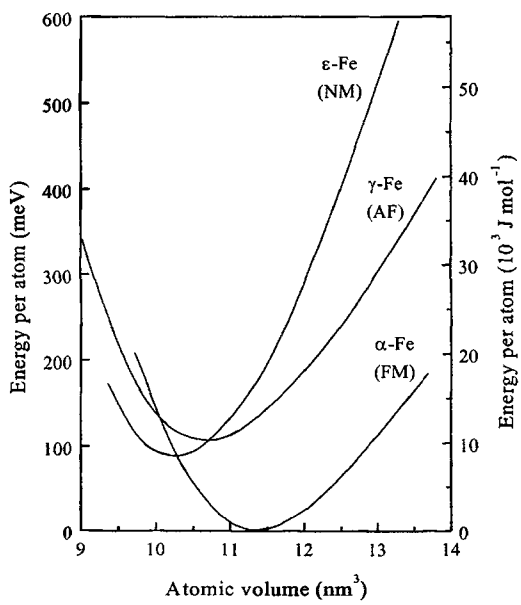

Figure 3. The comparison of ground state energies of α, γ and ϵ-Fe. Each phase is shown in the magnetic state of lowest energy. NM: nonmagnetic; AF: antiferromagnetic; FM: ferromagnetic

One can gain information on the specific heat of ϵ-Fe by extrapolating the concentration dependence of the properties of ϵ-Fe-Ru alloys to pure ϵ-Fe [16]. This allows the determination of G^{ϵ} and subsequently the differences in the Gibbs free energies of the ϵ and γ-phases as shown in figure 2b. From this figure it can be seen that the ϵ-phase is more stable than the γ-phase below about 400 K, which is in agreement with the value of 450 K found from the extrapolation in figure 1. α-Fe is always more stable than ϵ-Fe and thus the temperature dependence of $G^{\alpha}-G^{\epsilon}$ is similar to that of $G^{\alpha}-G^{\gamma}$.

3.2 The volume dependence of the total energy

The atomic volume dependence of the total energy of the ground states of α, γ and ϵ-Fe are shown in figure 3 [17]. Only the curves representing the magnetic state of lowest energy for each phase is shown. At T=0 α-Fe is most stable, followed by ϵ-Fe and then by γ-Fe. The calculated energy differences are larger than the corresponding ΔG by a factor of about 2. However, both give the same sequence for the stability of the different phases and, therefore, the thermodynamical considerations and the results of the total energy calculations are in good agreement.

4. THE GROUND STATE PROPERTIES OF ϵ-Fe

The magnetic moment and the total energy of ϵ-Fe were calculated by employing the full potential linearized augmented plane wave method, which is based on the density functional theory. The generalized gradient approximation (GGA) in the Perdew-Wang formula was used for the exchange-correlation potential [18]. All calculations were performed with the WIEN 95/97 [19].

In the ground state of ϵ-Fe the NM and AF states are nearly degenerate with $\mu \sim 0$ as observed in figure 4. Antiferromagnetism is more stable above 11.0×10^{-3} nm^3 where the magnetic moment is strongly volume dependent. At separations larger than 12.1×10^{-3} nm^3, a FM state with a large moment appears which is more stable than the AF state. The experimental points given in the plot give further support to the validity of the diagram and are itemized and discussed below.

1. The results of Mössbauer experiments on ϵ-Fe show that no magnetic ordering occurs at low temperatures (T=0.03 K) and pressures up to 21 GPa [20], so that $\mu = 0$ in agreement with the results given in Figure 4.

2. Fe can be accommodated in a hcp environment when alloyed with Ru or Os [21] which lie just below Fe in the periodic system, and also when alloyed with the neighboring elements Mn [22] and Ir [23]. The ternary systems Fe-Co-Mn [24] and Fe-Ni-Cr can also take up a hcp structure [25,26]. The ϵ-phase in these alloys is only found as a low temperature product phase of a martensitic phase transformation for which the parent phase is fcc. The transformation of the fcc structure to the denser packed hcp structure causes the atomic volume to decrease. However, some hcp Fe alloys order antiferromagnetically because of the lattice expansion caused by the alloying element. The ϵ-phase in Fe-Mn ranges between 10 to 28 at. % Mn. The Néel temperature T_N is about 230 K and the magnetic moment is about $0.25\,\mu_B$. Both are practically independent of composition in this range [27]. In Fe-Ru alloys the ϵ-phase occurs in the concentration range 12 – 35 at.% Ru [26] and the alloys are AF with a small moment of $\sim 0.1\,\mu_B$.

3. Although the ϵ-phase Fe alloys with Ru are in an AF state, a FM state is found for ϵ-Fe thin films grown epitaxially on hexagonal Ru. These films have a large atomic volume of $V_a = 12.5 \times 10^{-3}$ nm^3.

4. C and N atoms enter into interstitial octahedral sites and lead to a volume expansion. The hexagonal nitride Fe_3N, with a magnetic moment of $1.72\,\mu_B$ and $T_C = 500$ K is FM. An isostructural carbide with the

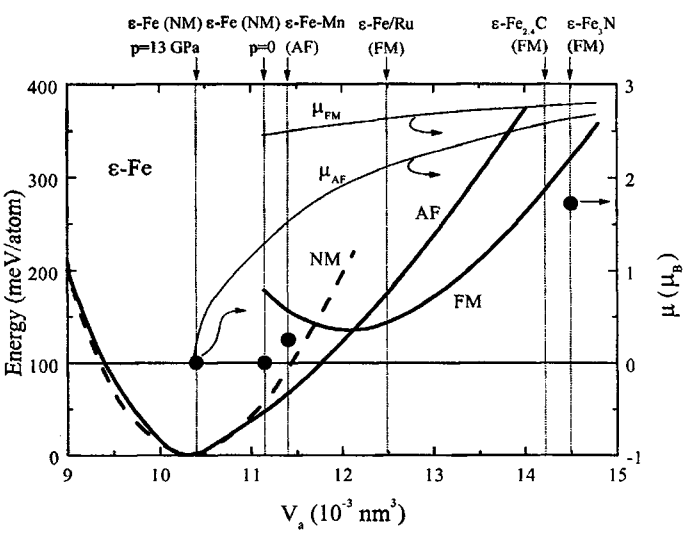

Figure 4. The atomic volume dependence of the total energy and magnetic moment of ϵ-Fe. The thick lines are the energy curves ●: experimental μ data (Tab. 1).

Table 1. Atomic volume and magnetic states of the various phases of ϵ-Fe.

Phase	V_a (10^{-3} nm^3)	μ (μ_B)	magnetic state
ϵ-Fe (p=13 GPa)	10.45	0	NM
ϵ-Fe (p=0)	11.15	0	NM
ϵ-$Fe_{78}Mn_{22}$	11.45	0.25	AF
ϵ-Fe/Ru (epitax.)	12.50		FM
ϵ-Fe_3N	14.56	1.72	FM
ϵ-$Fe_{2.4}C$	14.30		FM

composition $Fe_{2.4}C$ is also FM. with $T_C \sim 750$K. The volume per Fe atom is $\sim 14.3 \times 10^{-3}$ nm^3.

The experimentally determined atomic volumes and the magnetic states of the various ϵ-Fe phases are summarized in table 1 and are indicated by arrows in figure 4 to compare with the theoretical results. Experiment and theory find good agreement.

5. DISCUSSION

Although neither Fe nor Mn take up a hexagonal structure in their allotropy, ϵ-Fe-Mn alloys can be stabilized in a limited concentration region. In the light of the magnetic properties of ϵ-Fe we can give an account for the presence of this ϵ-phase. The structural and magnetic phase diagram of Fe-Mn is given in figure 5. M_s, M_f, A_s and A_f denote the martensite start, martensite finish, austenite start and austenite finish temperatures respectively. The concentration dependence of the Néel temperatures of the ϵ and γ-phases are drawn by heavy lines. The ϵ-phase ranges from about 10 to 28 at. % Mn, however it is either mixed with the α-phase or the γ-phase and the quantity of ϵ-phase that occurs depends on the thermal history of the sample.

The interesting fact is that the ϵ-phase begins to stabilize at a Mn concentration near the percolation limit. Below this limit Mn atoms are positioned essentially at next nearest neighbor positions amongst each

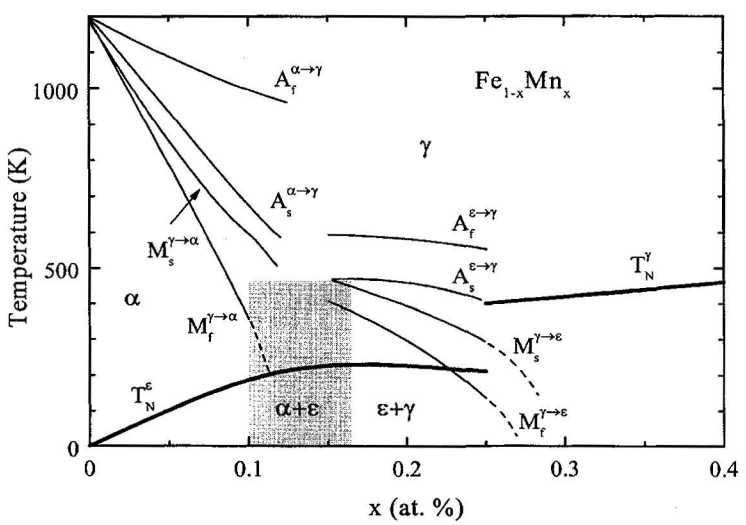

Figure 5. The structural and magnetic phase diagram of Fe-Mn allyos. The shaded area shows the ϵ-phase stability region.

other so that the Mn-Mn coupling is FM. Just below the percolation limit of about 14 at.% Mn-Mn pairs can occupy nearest neighbor position leading to AF coupling which tends to destroy the long range FM coupling of the Fe atoms. As discussed above within thermodynamical and theoretical considerations, the absence of FM coupling then leads to the stabilization of the ϵ-phase. Based on this premise it could be possible to manipulate the ϵ-stability range by alloying with appropriate elements that can hinder the ferromagnetism of α-Fe.

References

1. A. Sato, E. Chishima, K. Soma, T. Mori, Acta Metall. **30**, 1177 (1982).
2. T. Y. Hsu, Xu Zuyao, Mat. Sci. Eng. **A273-275**, 494 (1999).
3. W. Y. Jang, J. I. Han, K. K. Jee, S. H. Baik, J. W. Kang, M. C. Shin, J. Phys. IV France **7**, C5-447 (1997).
4. P. Marineli, A. Baruj, S. Cotes. A. F. Guillermet, M. Sade, Mat. Sci. Eng. **A273-275**, 498 (1999).
5. G. J. Arruda, V. T. L. Bruno, M. S. Andrade, Mat. Sci. Eng. **A273-275**, 528 (1999).
6. M. Acet, T Schneider, B. Gehrmann, E. F. Wassermann, J. Phys. IV Colloq. **C8**, C8-379 (1995).
7. H. M. Strong, R. E. Tuft, R. E. Hanneman, Metall. Trans. **4**, 2657 (1973).
8. L. Lin-Gun, W. A. Bassett, J. Geophys. Res. **80**, 3777 (1975).
9. L. K. Kaufman, E. V. Clougherty, R. J. Weiss, Acta Met. **11**, 223 (1963).
10. F. P. Bundy, J. Appl. Phys. **36**, 616 (1965).
11. P. M. Giles, M. H. Langenbach, A. R. Marder, J. Appl. Phys. **42**, 4290 (1971).
12. M Acet, H. Zähres, E. F. Wassermann, W. Pepperhoff, Phys. Rev. B **49**, (1994) 6012
13. M. Acet, E. F. Wassermann, W. Pepperhoff, Phil. Mag. B **80**, 127 (2000).
14. Kaufman, L. K., Clougherty, E. V., Weiss, R. J., Acta Met. **11**, 223 (1963).
15. Bendick, W., Pepperhoff, W., Acta Met. **30**, 679 (1982).
16. L. Kaufmann, H. Bernstein *Computer Calculations of Phase Diagrams* (Academic Press, New York, 1970) p.18.
17. H. C. Herper, E. Hoffmann, P. Entel, Phys. Rev. B **60**, 3839 (1999).
18. J. P. Perdew and Y. Wang, Phys. Rev. B **45**, 13244 (1992).
19. P. Blaha, K. Schwarz, P. Soratin, S. B. Trickey, Comput. Phys. Commun. **59**, 399 (1990).
20. G. Cort, R. D. Taylor, J. O. Willis, J. Appl. Phys. **53**, 2064 (1982).
21. L. D. Blackburn, L. Kaufmann, M. Cohen, Acta Met. **13**, 533 (1965).
22. H. Schumann, Z. Metallkde. **58**, 207 (1967).
23. M. Miyagi, C. M. Wayman, Trans. Metallurg. Soc. AIME **236**, 806 (1966).
24. G. Benkissen, L. J. Lyssak, B. J. Nikolin, H. Schumann, Neue Hütte **25**, 326 (1980).
25. P. M. Kelly, Acta Met. **13**, 635 (1965).
26. H. Schumann, Technik **23**, 242 (1968).
27. H. Ohno, M. Mekata, J. Phys. Soc. Japan **11**, 102 (1971).